

EVALUATION OF ANTI-HYPERGLYCEMIC EFFECT OF SYNTHETIC SCHIFF BASE VANADIUM(IV) COMPLEXES

F. A. El-Saied,^{1, 2} T. A. Salem,³ S. A. Aly,⁴ and M. M. E. Shakhdofa^{5, 6, *}

Original article submitted December 9, 2016.

A chain of new vanadium(IV) complexes of Schiff bases, derived from acetohydrazide (HL¹⁻³) or 4-aminoantipyrine (HL⁴⁻⁷) have been prepared and physicochemically distinguished using different tools including analytical, spectral, and magnetic techniques. The spectral and analytical data showed that ligands HL¹⁻³ acted as neutral bidentate ligands, chelated through hydrazono carbonyl and azomethine groups, whereas HL⁴ acted as neutral tetradentate ligand coordinated via pyrazolone carbonyl, NH group, hydrazono carbonyl, and azo (N=N) groups forming binuclear complexes. The HL⁵ and HL⁶ behave as neutral bidentate ligands coordinating through pyrazolone carbonyl and NH groups; in case of ligand HL⁶, in addition to the mentioned mode, C=N and C≡N groups participated to bind a second VO(II) ion form binuclear complexes. HL⁷ behaves as a monobasic bidentate ligand bonded via deprotonated OH and azomethine groups. All complexes adopt square pyramidal geometry around vanadium ion. Results revealed that the oral management of vanadium complexes significantly reduced the blood glucose level in rats suffered from diabetes. The correction of altered biochemical parameters via treatment with vanadium complexes points the improved glucose balance.

Key words: vanadium complexes; anti-diabetic activity; antipyrine; acetohydrazide.

1. INTRODUCTION

The diabetes mellitus (DM) prevalence is rapidly emerging at a horrifying ratio and is deemed to be one of the most valid troubles in the world leading to significant veracity and economic burden on sick person and society [1]. DM is distinguished by chronic hyperglycemia that gives rise to the troubles in metabolism of carbohydrates, proteins and lipids with a rising hazard of cachexy and death rate from elementary in addition to subaltern complexities [2]. DM is usually subdivided into insulin-dependent (type 1) and non-insulin dependent (type 2). Type 1 DM is controllable via insulin daily injections, while type 2 DM is usually treated by many kinds of synthetic drugs [3]. Hence, researchers continue in

preparing novel drugs possessing efficient antidiabetic activity at tiny concentrations without side effects.

Vanadium is a transition element which is suggested to be a fundamental trace element in humans and animals. Vanadium compounds have been demonstrated to possess antidiabetic properties and insulin-mimetic activity in animal models of DM type 1 and 2, in addition to a small number of diabetic humans subjected to treatment by these compounds [4 – 7]. These complexes also have considerable versatility in modulation of pharmacological properties [8]. However, the potential antidiabetic activity of most complexes derived from vanadium so far was studied for compounds poorly absorbed in their inorganic forms, which needed high doses and were accompanied with unfavorable side effects. Because of the toxicity of vanadium inorganic salts, various organovanadium complexes have been synthesized and screened for their antidiabetic effectiveness [9]. The modern stage in studying antidiabetic properties of vanadium began in 1985 by works of John McNeill with coworkers. They investigated the heart function of rats with streptozotocin (STZ) induced diabetes after treatment with vanadium(IV) sulfate [10]. Previously, insulin-like effects of vanadium salts were reported in cells systems such as adipocytes [11]. The STZ diabetic rat model is now widely used to study the *in vivo* effects of vanadium compounds. STZ-induced diabetes is considered a

¹ Department of Chemistry, College of Science, Qassim University, KSA.

² Department of Chemistry, Faculty of Science, El-Menoufia University, Shebin El-Kom, Egypt.

³ Department of Biochemistry, College of Medicine, Qassim University, KSA.

⁴ Genetic Engineering and Biotechnology Research Institute, El Menoufia University, Sadat City, Egypt.

⁵ Department of Chemistry, Faculty of Sciences and Arts, Khulais, University of Jeddah, Saudi Arabia.

⁶ Inorganic Chemistry Department, National Research Centre, P. O. 12622 Dokki, Cairo, Egypt.

* e-mail: mshakhdofa@gmail.com

type 1 DM model, since it arises from destruction of some, but not all, of the insulin-producing pancreatic β -cells [12].

In this context, the present work was aimed to synthesize novel vanadium complexes of 2-(phenylamino)-*N'*-(pyridin-2-ylmethylene)acetohydrazide (HL¹), 2*N'*-(furan-2-ylmethylene)-2-(phenylamino)acetohydrazide (HL²), *N'*-(2-hydroxybenzylidene)-2-(phenylamino)acetohydrazide (HL³), (2-cyano-*N*-(1,5-dimethyl-3-oxo-2-phenyl-2,3-dihydro-1H-pyrazol-4-yl)-2-(phenyldiazenyl)acetamide (HL⁴), 2-cyano-*N*-(1,5-dimethyl-3-oxo-2-phenyl-2,3-dihydro-1H-pyrazol-4-yl)-2-(*m*-tolyl diazenyl)acetamide (HL⁵), (1,5-dimethyl-3-oxo-2-phenyl-2,3-dihydro-1H-pyrazol-4-yl)carbonohydrazonoyl dicyanide (HL⁶), and 2-cyano-*N'*-((1,5-dimethyl-3-oxo-2-phenyl-2,3-dihydro-1H-pyrazol-4-yl)methylene)-2-(phenyldiazenyl)acetohydrazonic (HL⁷) ligands. The obtained metal complexes were characterized by various spectral techniques. The antidiabetic properties of these complexes were assessed on STZ-induced diabetes model in rats.

2. EXPERIMENTAL

2.1. Materials

The chemicals and reagents used for the synthesizing of the chelates and their VO(II) coordination compounds were of analytical grade and used without further purification. Ethyl [2-(phenylamino)]acetate and 2-(phenylamino)acetohydrazide were synthesized by a published method [13 – 15].

2.2. Synthesis of Schiff Base Ligands

The Schiff base ligands 2-(phenylamino)-*N'*-(pyridin-2-ylmethylene)acetohydrazide (HL¹), 2*N'*-(furan-2-ylmethylene)-2-(phenylamino)acetohydrazide (HL²), and *N'*-(2-hydroxybenzylidene)-2-(phenylamino)acetohydrazide (HL³) were synthesized by mixing 2-(phenylamino)acetohydrazide with 2-pyridinealdehyde (HL¹), 2-furaldehyde (HL²) and 2-hydroxybenzaldehyde (HL³) at 1 : 1 molar ratio in 50 mL absolute ethyl alcohol. The mixtures were refluxed for 3 h and the solid products were filtered off, washed with ethanol, recrystallized from ethyl alcohol, and dehydrated over anhydrous CaCl₂ [13 – 15]. The ligands (2-cyano-*N*-(1,5-dimethyl-3-oxo-2-phenyl-2,3-dihydro-1H-pyrazol-4-yl)-2-(phenyldiazenyl)acetamide (HL⁴) and 2-cyano-*N*-(1,5-dimethyl-3-oxo-2-phenyl-2,3-dihydro-1H-pyrazol-4-yl)-2-(*m*-tolyl diazenyl)acetamide (HL⁵) were obtained by coupling 2-amino-2-cyano-*N*-(1,5-dimethyl-3-oxo-2-phenyl-2,3-dihydro-1H-pyrazol-4-yl)acetamide with aniline and *m*-toluidine, respectively, in pyridine. The product was recrystallized several times from ethanol [16]. Ligand (1,5-dimethyl-3-oxo-2-phenyl-2,3-dihydro-1H-pyrazol-4-yl)carbonohydrazonoyl dicyanide (HL⁶) was prepared by coupling the diazonium salt of 4-aminoantipyrine with malononitrile in sodium hydroxide [17]; 2-cyano-*N'*-((1,5-dimethyl-3-oxo-2-phenyl-2,3-dihydro-1H-pyrazol-4-yl)methylene)-2-(phenyldiazenyl)acetohydrazonic (HL⁷) was prepared by coupling the

diazonium salt of aniline with 4-formylcyanoacetohydrazide antipyrine in sodium hydroxide solution [17].

2.3. Synthesis of VO(II) Complexes

Vanadyl VO(II) complexes (**1 – 7**) were synthesized by mixing a hot ethyl alcohol solution of VOSO₄·3H₂O (in the presence of 2 mL distilled H₂O) with the appropriate amount of hot ethyl alcohol solution of the corresponding ligand using in 1L : 1M molar ratio. The reaction mixtures were refluxed for 3 h and the precipitated products were filtered off, washed several times with ethyl alcohol, and dehydrated in vacuum desiccators on top of anhydrous CaCl₂.

2.4. Physical Measurements

Elemental analyses of all compounds were carried out on a micro-analytical unit (Cairo University, Egypt). Perkin-Elmer 683 infrared spectrophotometer covering a wavelength range of 200 – 4000 cm⁻¹ was used to record the IR spectra of all compounds in KBr disks. Perkin-Elmer 550 spectrophotometer was used to record the electronic absorption spectra in a 200 – 900 nm regions. The Gouy method was used to measure the magnetic susceptibilities at 25°C, with mercuric tetrathiocyanatocobaltate(II) as the magnetic susceptibility standard. Diamagnetic corrections were estimated using Pascal's constant [18]. The magnetic moments were calculated using the following equation:

$$\mu_{\text{eff}} = 2.84 \sqrt{\chi_M^{\text{corr}} T}$$

2.5. Evaluation of Anti-Hyperglycemic Activity of VO(II) Complexes

2.5.1. Preparation of solutions of vanadium complexes. Seven newly synthesized vanadium complexes were freshly dissolved (w/v) in 60% DMSO immediately before use. Experimental animals orally received test compounds in a dose of 1 mg/kg/day for 4 weeks.

2.5.2. Induction of experimental diabetes. Experimental diabetes was induced in male Wistar rats weighing 160 – 180 g by intraperitoneal injection of 60 mg/(kg B. W.) of STZ dissolved in 0.1 M cold citrate buffer pH 4.5 [19]. On the 3rd day, the development and aggravation of diabetes in rats was confirmed and rats with fasting blood glucose concentration above 250 mg/dL were selected for the experiments [20]. The experiments were designed and conducted in strict accordance with the current ethical norms approved by the Animal Ethical Committee guidelines. The rats were divided into six groups (each comprising six animals) as follows: (Group 1) normal rats; (Group 2) STZ-induced diabetes rats; (Groups 3, 4, 5, 6, 7, 8, and 9) diabetic rats treated orally with vanadium complexes 1, 2, 3, 4, 5, 6, and 7, respectively (1 mg/(kg B. W.)/rat/day) for 4 weeks.

2.5.3. Biochemical analysis. At the end of experiment, rats were fasted overnight, anaesthetized by diethyl ether, and sacrificed by cervical decapitation. Blood was collected with and without anticoagulant for plasma and serum separa-

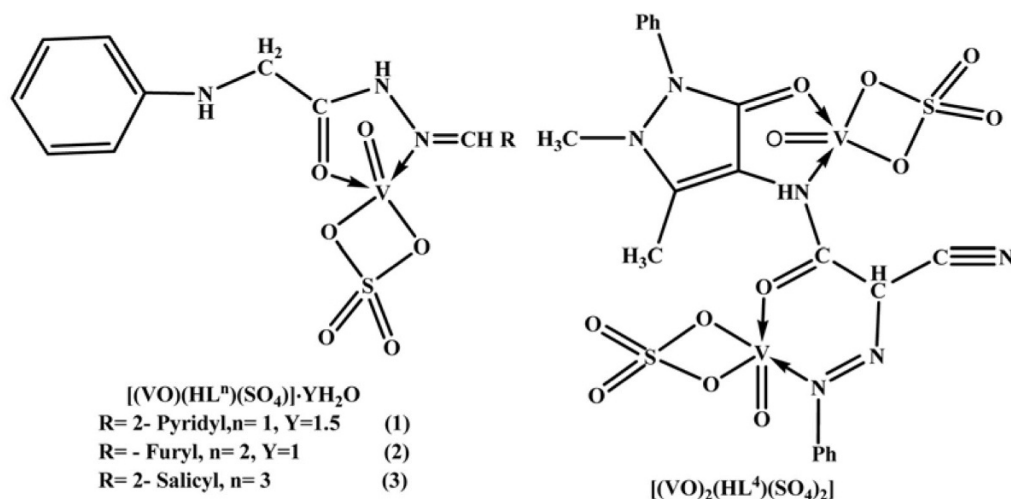


Fig. 1. Chemical formulas of VO(II) complexes 1 – 4.

tion, respectively. Fasting blood glucose, plasma insulin, plasma protein, blood urea and serum creatinine were estimated according to the manual instructions in the corresponding kits. The activities of ALT, AST and ALP in serum were assayed according to the kit procedure. Liver tissues were excised out, washed with ice-cold saline, and liver homogenates were prepared for glycogen, reduced glutathione, and lipid peroxidation estimations.

2.5.4. Determination of plasma insulin. Insulin levels in rat plasma were quantified by ELISA (Merckodia, Sweden). Briefly, plasma insulin was captured by pre-titrated amount of a monoclonal mice anti-rat insulin antibodies and the binding of biotinylated polyclonal antibodies to the captured insulin. After washing, horseradish peroxidase

(HRP) was titrated and washed for 5 times. The immobilized antibody-enzyme conjugates were quantified by monitoring HRP activities in the presence of substrate 3,3',5,5'-tetramethylbenzidine. The enzyme activity was measured spectrophotometrically at 450 nm.

Determination of hepatic glycogen. Glycogen was isolated by digesting the liver slices with 1 mL of 30% (w/v) KOH in a boiling-water bath for 30 min. Then, 0.1 mL of 2% (w/v) Na_2SO_4 and 3 vol. of ethanol were added to precipitate the glycogen. The isolated glycogen was determined by the method of Roe and Daily [21].

2.5.6. Estimation of hepatic oxidative markers. The level of reduced glutathione (GSH) in liver homogenate was estimated using the method described by Beutler, et al. [22].

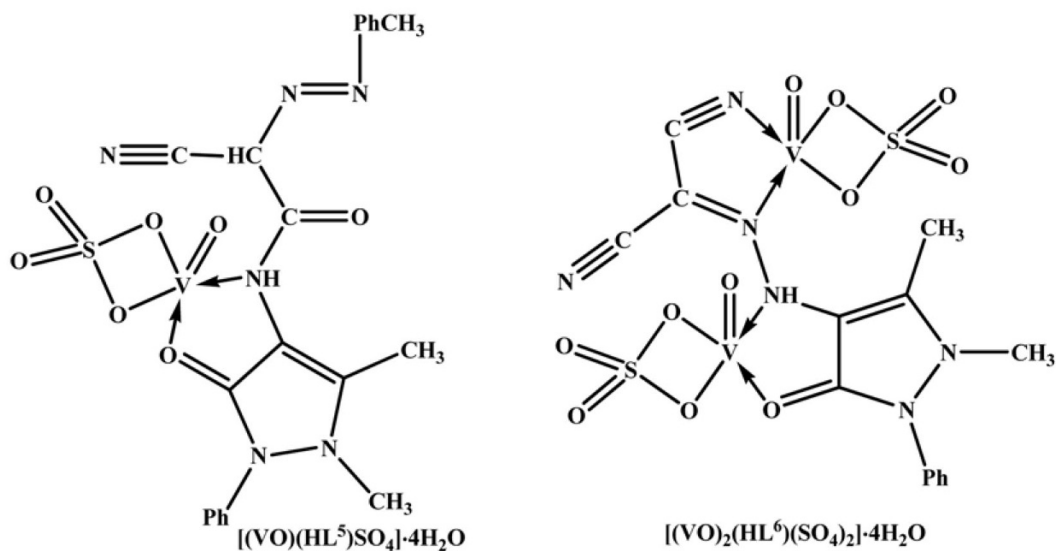


Fig. 2. Chemical formulas of VO(II) complexes 5 and 6.

Hepatic lipid peroxide was determined by the thiobarbituric acid (TBA) reaction as described by Ohkawa, et al. [23].

2.5.7. Estimation of hepatic glucokinase activity. One gram of fresh liver tissue was homogenized with 9 mL Tris-KCl-EDTA buffer and centrifuged at 15000 rpm for 1 h at 4°C. Twenty five microliters of clear supernatant was used for glucokinase assay according to the method of Jamdar and Greengard [24].

2.5.8. Statistical analysis. All data were grouped and statistically evaluated with MS Excel software. All values were presented as means \pm SE (standard error). Comparisons among groups were made by application of two-way analysis of variance (ANOVA) followed by one-way ANOVA and post hoc analysis. Differences were considered statistically significant if $p < 0.05$.

3. RESULTS AND DISCUSSION

The reactions of the ligands *N'*-[(2-pyridine-2-yl-methylene)2-(phenylamino)] acetohydrazide (HL¹), *N'*-[(2-furan-2-yl-methylene)2-(phenylamino)]acetohydrazide (HL²), *N'*-[(2-hydroxybenzyl-2-yl-methylene)2-(phenylamino)] acetohydrazide (HL³), 4-azocyanacetamidoaniline antipyrine (HL⁴), 4-azocyanacetamido-*m*-toluidine (HL⁵), 4-azomalonitrile antipyrine (HL⁶) and 4-formylazohydrozoaniline antipyrine (HL⁷) with VOSO₄·3H₂O at equal molar ratio (1:1) led to the formation of metal complexes 1–7 with structures displayed in Figs. 1–3. All the compounds appear as brown or green colored crystalline solids stable at room temperature (RT). The complexes are insoluble in polar and non-polar solvents but soluble in polar coordinating solvents such as DMSO and DMF. The physicochemical and spectroscopic data summarized in Tables 1–3 confirm that complexes have structures shown in Figs. 1–3.

The results of elemental analyses (Table 1) showed that complexes 1–5 were mononuclear 1 : 1 metal complexes, whereas compound 6 was a binuclear complex and compound 7 was 2 : 1 metal complex (L : M). The molar conduc-

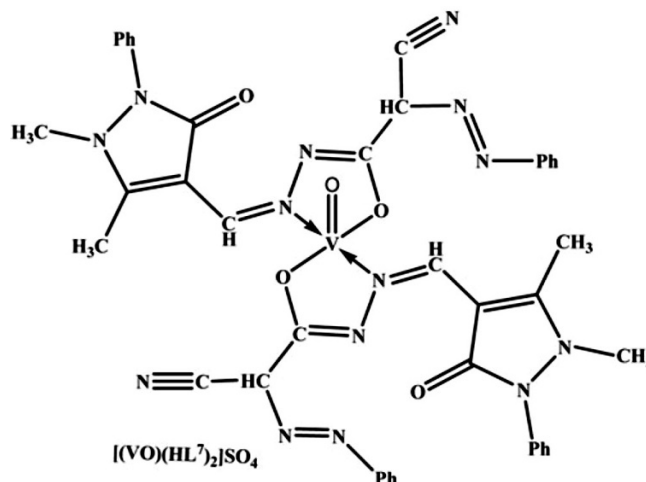


Fig. 3. Chemical formula of VO(II) complex 7.

tivities of 1×10^{-3} M solutions of metal complexes 1–6 in *N,N*-dimethylformamide (DMF) at RT were in the 6.8–17.1 $\Omega^{-1} \text{ cm}^2 \text{ mol}^{-1}$ range indicating the non-electrolytic nature of these complexes (Table 1). These data confirm that the sulfate groups are directly attached to the metal ion. However, complex 7 has a conductivity of $72.7 \Omega^{-1} \text{ cm}^2 \text{ mol}^{-1}$, which is indicative of the electrolytic nature of this complex. This conclusion agrees with data of Greenwood, et al. [25], which reported the interval of 50–70 $\Omega^{-1} \text{ cm}^2 \text{ mol}^{-1}$ for 1 : 1 electrolyte in DMF.

3.1. Infrared Spectra

The ligand binding modes in complexes have been concluded from the IR spectroscopy data. The most diagnostic IR absorption peaks of all compounds are listed in Table 2. The spectra of complexes HL¹–HL³ revealed bands at 3390–3363, 3211–3185, 1698–1672, and 1603–1585 cm^{-1} . The first two bands were assigned to $\nu(\text{NH})$ and

TABLE 1. Analytical and Physicochemical Data for VO(II) Complexes

No.	Complex	Color	Found (Calculated), %			^a Λ_m
			C	H	N	
1	[(VO)(HL ¹)(SO ₄)] · 1.5H ₂ O	Brown	37.9(37.8)	3.8(5.8)	13.2(12.9)	–
2	[(VO)(HL ²)(SO ₄)] · H ₂ O	Brown	36.8(36.7)	3.9(3.8)	9.6(9.9)	17.1
3	[(VO)(HL ³)(SO ₄)]	Green	41.3(41.7)	3.3(3.5)	9.8(9.7)	14.0
4	[(VO) ₂ (HL ⁴)(SO ₄) ₂]	Green	34.5(34.2)	3.1(2.7)	11.8(12.0)	6.8
5	[(VO)(HL ⁵)(SO ₄)] · 4H ₂ O	Brown	40.2(40.5)	5.0(4.5)	13.6(13.5)	15.0
6	[(VO) ₂ (HL ⁶)(SO ₄) ₂]	Brown	26.9(27.7)	2.1(2.0)	14.2(13.9)	16.5
7	[(VO)(HL ⁷) ₂ (SO ₄)]	Brown	51.9(52.2)	4.2(3.9)	20.3(20.9)	72.7

^a Molar conductivity of 10^{-3} M solutions ($\text{ohm}^{-1} \text{ cm}^2 \text{ mol}^{-1}$).

the other two peaks were attributed to carbonyl and azomethine groups, respectively. The IR spectra of complexes **1** – **3** showed that the peaks related to azomethine and carbonyl groups appeared at lower wavenumbers compared to those of the free ligands, suggesting their chelation to the VO(II) ion. The spectra of complexes also showed that the peaks related to $\nu(\text{NH})$ were slightly shifted relative to those of the ligands as a result of the coordination of neighboring groups. The spectrum of ligand HL³ displayed a peak at 3364 cm⁻¹, which referred to $\nu(\text{OH})$. This band appeared at the same position for complex **3**, indicating that the OH group did not participate in the chelation.

The IR spectra of HL⁴ – HL⁷ displayed bands at 3397 – 3384, 3250 – 3204, and 2210 – 2205 cm⁻¹. The first two bands were assigned to $\nu(\text{NH})$ and the one referred to cyano group. The spectrum of HL⁶ revealed another peak at 2362 cm⁻¹ assigned to the second cyano group. In addition, the IR spectra of HL⁴ – HL⁷ showed bands at 1645 – 1630 cm⁻¹ assigned to carbonyl groups of the pyrazolone ring. The spectra of HL⁴ and HL⁵ revealed a peak at 1687 – 1661 cm⁻¹ referred to carbonyl groups of the hydrazone moiety. The spectrum of HL⁷ did not show a peak characteristic of carbonyl groups of the hydrazone moiety, but two additional bands appeared at 1605 and 1585 cm⁻¹ and referred to $\nu(\text{C}=\text{N}-\text{N}=\text{C}-)$, indicating that the ligand exists in its enole form. The spectrum of HL⁶ revealed a peak at 1587 cm⁻¹ assigned to azomethine linkage. The IR spectra of HL⁴, HL⁵ and HL⁷ ligands displayed a band at 1490 – 1482 cm⁻¹ that referred to azo linkage. The IR spectrum of binuclear complex [(VO)₂(HL⁴)(SO₄)₂] (**4**) revealed characteristic peaks of

amino and carbonyl groups of the pyrazolone ring, carbonyl of hydrazone moiety, and azo linkage, which appeared at lower wavenumbers as compared to those of the free ligand as a result of their participation in the coordination to vanadyl ion. This spectrum also revealed that the peak related to cyano linkage appears at the same location as in the spectrum of free ligand, indicating that it does not participate in the coordination.

The above discussion suggests that a ligand in the complex comprises two compartments: the first compartment bonded to the vanadyl ion via the pyrazolone carbonyl group and the –NH group, and the second compartment bonded to the second vanadyl ion via the N=N and hydrazone carbonyl groups. The rest part of coordination number 5 is satisfied by the bidentate sulfate. The IR spectrum of complex [(VO)(HL⁵)SO₄·4H₂O] (**5**) reveals that the peaks related to amino and carbonyl groups of pyrazolone ring appear at lower wavenumbers as compared to those for the ligand, indicating that coordination take place via the NH and C=O groups of the pyrazolone ring. This spectrum also displays peaks related to $\nu(\text{C}\equiv\text{N})$, $\nu(\text{C}=\text{O})$ of hydrazone moiety, and $\nu(\text{N}=\text{N})$, which appear at the same wavenumbers as those for the free ligand, showing that these groups do not take part in coordination. The HL⁵ ligand in this complex behaved as a neutral bidentate ligand coordinated through NH group and carbonyl oxygen atom of the pyrazolone ring. The IR spectrum of complex [(VO)₂(HL⁶)(SO₄)₂] (**6**) reveals that peaks related to the carbonyl of hydrazone moiety and $\nu(\text{NH})$ appear at higher wavenumbers as a result of their coordination, whereas the bands ascribed to one cyano group and

TABLE 2. IR Absorption Bands and Their Assignments in the Spectra of Ligands and Their VO(II) Complexes

No.	$\nu(\text{OH})/\text{H}_2\text{O}$	$\nu(\text{NH})$	$\nu(\text{C}=\text{N})$	$\nu(\text{C}=\text{O})^a$	$\nu(\text{C}=\text{O})^b$	$\nu(\text{C}=\text{N})$	$\nu(\text{N}=\text{N})$	$\nu(\text{SO}_4)$	$\nu(\text{V}=\text{O})$	$\nu(\text{V}-\text{O})$	$\nu(\text{V}-\text{N})$
HL ¹	–336	3211	–	–	1698	1603	–	–	–	–	–
1	3417	3270	–	–	1660	1590	–	1130,1041	977	605	510
HL ²	–	3390,3324, 3185	–	–	1672	1585	–	–	971	–	–
2	3432	3324,3188	–	–	1628	1520	–	1124,1050	979	615	510
HL ³	3364	3187	–	–	1691	1603	–	–	–	–	–
3	3368	3280	–	–	1611	1541	–	1139,1050	981	620	502
HL ⁴	–	3397	2206	1644	1687	–	1482	–	–	–	–
4	–	3100	2207	1625	1661	–	1475	1149, 1050	989	602	503
HL ⁵	–	3384, 3204	2210	1645	1661	–	1488	–	–	–	–
5	3435	3221	2209	1605	1660	–	1488	1165,1038	971	623	489
HL ⁶	–	3200	2205, 2362	1630	–	1587	–	–	–	–	–
6	–	3440	1185,2360	1638	–	1568	–	1130,1045	976	607	510
HL ⁷	3430	–	2360	1645	–	1605,1585	1490	–	–	–	–
7	3410	–	2358	1645	–	1603,1552	1494	1152,1009	981	603	520

^a $\nu(\text{C}=\text{O})$ of pyrazolone ring; ^b $\nu(\text{C}=\text{O})$ of hydrazine.

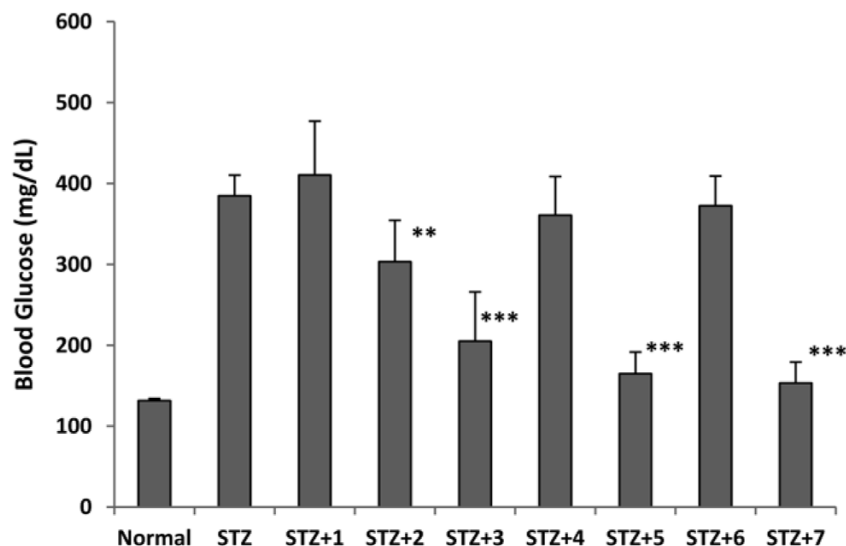


Fig. 4. Effect of vanadium complexes on the blood glucose level in rats with STZ-induced diabetes: (*) significant, (**) high significant, (***) very high significant differences in comparison to diabetic rats.

azomethine group appear at lower wavenumbers as compared to those for the free ligand, indicating that they participate in coordination to the vanadyl ion. Moreover, the second $\nu(\text{C}\equiv\text{N})$ peak does not show any shift relative to that for the free ligand. The IR spectrum of complex $[(\text{VO})(\text{HL}^7)_2(\text{SO}_4)]$ (**7**) shows that the band characteristic of $\nu(\text{OH})$ is shifted to lower wavenumbers as a result of coordination. The band at 1603 cm^{-1} remains at the same position, while the band observed at 1585 cm^{-1} in the spectrum of ligand appears at a lower wavenumber (1552 cm^{-1}) for the complex, indicating that HL^7 ligand is coordinated in its enol form via $-\text{C}=\text{N}$ and OH group. This is also supported by the disappearance of a band characteristic of the carbonyl of hydrazone moiety. This spectrum also displays the peaks related to cyano, carbonyl, and azo linkage without any shift, indicating that they do not take part in chelation. The IR spectra of vanadyl complexes reveal two new peaks in the regions of $1165-1124$ and $1041-1138\text{ cm}^{-1}$, referred to coordinated sulfate group as a

bidentate ligand. The spectra of all vanadyl complexes show three new bands at $989-971$, $623-602$, and $520-502\text{ cm}^{-1}$, which are attributed to $\nu(\text{V}=\text{O})$ [26], $\nu(\text{V}-\text{O})$, and $\nu(\text{V}-\text{N})$, respectively [27]. The spectra of complexes **1**, **2**, and **5** show a broad peak at $3435-3417\text{ cm}^{-1}$ assigned to stretching vibrations of the molecules of water of hydration.

3.2 Electronic Absorption Spectra and Magnetic Moments

The electronic absorption spectra of $\text{VO}(\text{II})$ complexes were recorded in Nujol mull. The characteristic spectral band wavenumbers and values of magnetic moment per metal ion measured at room temperature are listed in Table 3. As can be seen from these data, the spectra of $\text{VO}(\text{II})$ complexes exhibit a band at $840-760\text{ nm}$, assigned to ${}^2\text{B}_2 > {}^2\text{E}(\nu_1)$ in a square pyramidal configuration [28]. The presence of a bands near 980 cm^{-1} in the IR spectra of all complexes and the their brown to green colors provide good evidence for the proposed structure. The values of magnetic moments (μ_{eff}) per metal ion in Table 3 are consistent with the presence of one electron and ruled out any exchange interactions between vanadium ions.

3.3 Evaluation of Anti-Hyperglycemic Activity of $\text{VO}(\text{II})$ Complexes

The *in vivo* effects of vanadium complexes were studied using STZ-induced diabetes model in rats. The STZ-induced diabetes is believed to be type 1 DM model since it emerges from demolition of the insulin producing pancreatic β cells [29]. Figure 4 shows the blood glucose levels of control and experimental groups of rats. The diabetic rats showed a marked increase ($P < 0.001$) in glucose level as compared to that in the control groups. The treatment of diabetic rats with various vanadium complexes led to different effects on the

TABLE 3. Electronic Absorption Bands in the Solid State and Room-Temperature Magnetic Moments of $\text{VO}(\text{II})$ Complexes

No.	Complex	<i>d-d</i> bands	μ_{eff} , βM (per metal ion)
1	$[(\text{VO})(\text{HL}^1)(\text{SO}_4)] \cdot 1.5\text{H}_2\text{O}$	765	1.9
2	$[(\text{VO})(\text{HL}^2)(\text{SO}_4)] \cdot \text{H}_2\text{O}$	760	1.87
3	$[(\text{VO})(\text{HL}^3)(\text{SO}_4)]$	820	1.95
4	$[(\text{VO})_2(\text{HL}^4)(\text{SO}_4)_2]$	840	2.05
5	$[(\text{VO})(\text{HL}^5)(\text{SO}_4)] \cdot 4\text{H}_2\text{O}$	810	2.03
6	$[(\text{VO})_2(\text{HL}^6)(\text{SO}_4)_2]$	817	1.79
7	$[(\text{VO})(\text{HL}^7)_2] \cdot \text{SO}_4$	833	1.83

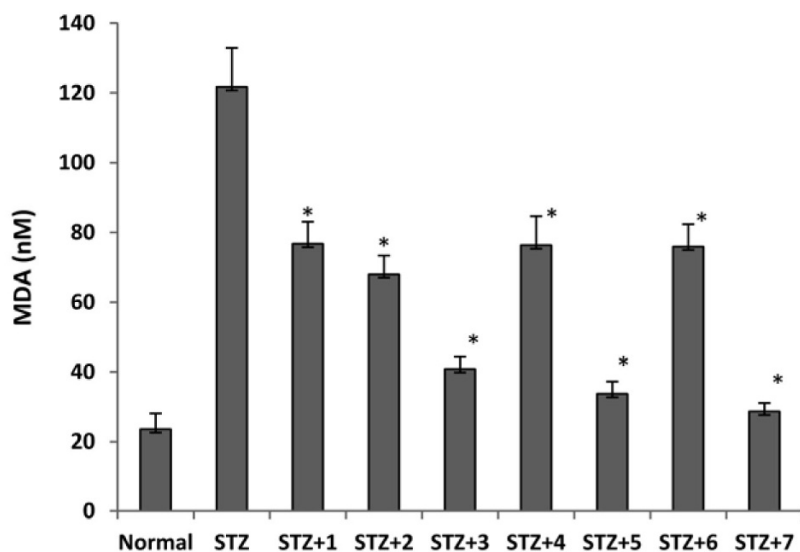


Fig. 5. Effect of vanadium complexes on the hepatic MDA level in rats with STZ-induced diabetes (*significant difference in comparison to diabetic rats).

blood glucose level. Significant decrease in the level of glucose in blood at fasting ($P < 0.001$) was found in diabetic rats treated with complexes **2**, **3**, **5**, and **7** as compared to the untreated diabetic group. There was no important variation in the blood glucose level in rats treated with vanadium complexes **1**, **4**, and **6**. Nevertheless, normal rats treated with the complexes did not show any significant change in fasting blood glucose level (data not presented here).

Table 4 presents data on the AST, ALT and ALP activity levels in serum of the control and experimental groups of rats. Results show that the activities of AST, ALT and ALP in serum of rats with STZ-induced diabetes were markedly increased ($P < 0.001$) as compared to values in the control. The elevated activity of AST, ALT and ALP significantly decreased ($P < 0.001$) in diabetic rats administered with vana-

dium complexes. A reduction in the levels of activity of AST ($P < 0.01$), ALT ($P < 0.001$) and ALP ($P < 0.01$) was observed in the diabetic rats treated with complexes **3**, **5** and **7**. At the same time, there was no significant alteration in the levels of activity of these enzymes in diabetic rats treated with other vanadium complexes in comparison to diabetic rats. Under normal physiological conditions, the activity of AST, ALT and ALP enzymes in serum is low and increases during tissue damage. A rise in the AST and ALT activity is indicative of hepatocellular damage. Further, ALP is a marker of biliary function and cholestasis. The observed increase in activities of these enzymes in the serum of diabetic rats may be due to the leakage of these enzymes from the liver cytosol into blood stream as a consequence of the hepatic tissue damage [30]. A significant reversal in AST,

TABLE 4. Effect of Vanadium Complexes on the Liver and Kidney Functions in Rats with STZ-Induced Diabetes

Group	ALT (U/L)	AST (U/L)	ALP (U/L)	Creatin. (mg/dL)	Urea (mg/dL)	TP (g/dL)
Normal	82.2 ± 3.1	113.4 ± 4.8	128.2 ± 11.3	0.5 ± 0.10	33.1 ± 5.9	8.45 ± 2.2
STZ	175.4 ± 9.8	198.5 ± 10.3	254.7 ± 16.7	1.6 ± 0.34	69.6 ± 8.3	4.71 ± 1.1
STZ+1	171.4 ± 8.9	201.2 ± 14.4	255.7 ± 21.3	1.7 ± 0.23	71.7 ± 6.5	3.96 ± 1.2
STZ+2	169.3 ± 7.6	196.7 ± 11.2	234.8 ± 23.1	1.4 ± 0.42	66.9 ± 7.5	4.21 ± 0.9
STZ+3	92.1 ± 5.7*	121.4 ± 10.4*	162.6 ± 11.5*	0.35 ± 0.04*	38.9 ± 6.3*	7.87 ± 1.5*
STZ+4	171.2 ± 10.1	189.8 ± 14.3	263.5 ± 23.5	1.41 ± 0.32	66.9 ± 7.2	3.31 ± 0.5
STZ+5	89.3 ± 7.8*	114.5 ± 9.7*	144.5 ± 13.5*	0.44 ± 0.06*	40.7 ± 7.6*	8.21 ± 1.3*
STZ+6	159.9 ± 9.9	198.7 ± 9.8	251.7 ± 20.3	1.61 ± 0.31	72.8 ± 3.5	4.30 ± 1.1
STZ+7	77.8 ± 6.5*	124.6 ± 6.5*	152.7 ± 17.3*	0.38 ± 0.07*	36.7 ± 7.6*	7.98 ± 2.1*

(*) Significant difference in comparison to diabetic rats.

ALT and ALP activities in diabetic rats treated with vanadium complexes is indicative of the tissue-protective character of these complexes.

In addition, Table 4 shows data on the plasma protein, blood urea, and serum creatinine levels in control and experimental groups of rats. The increased levels of urea and creatinine and reduced levels of total protein in rats with STZ-induced diabetes were significantly improved ($P < 0.001$) after treatment with vanadium complexes **3**, **5**, and **7** for four weeks. Normal rats treated with these complexes showed no significant changes in indicated parameters (data not shown). Insulin deprivation in diabetic milieu causes a profound increase in protein catabolism. Moreover, protein catabolism during diabetes is due to a net increase in protein breakdown rather than a decline in protein synthesis [31]. The imbalance between synthesis and catabolism of protein can have remarkable consequences in the metabolism of many tissues such as gut, skeletal muscles, and heart [32]. The anti-diabetic property of vanadium complexes may account for the observed increase in the levels of plasma proteins in diabetic rats treated with the complexes. Urea is the main end product of protein catabolism in the body. Under the DM conditions, the pronounced degradation of both hepatic and plasma proteins leads to the excessive accumulation of urea in the systemic circulation in comparison to excretion. During diabetes, damages occur in tissues such as kidney due to the elevated supra-physiological concentration of glucose, causing impairment in the renal function and resulting in the accumulation of nitrogenous wastes in the circulation system. This in turn elevates the urea and creatinine levels in the blood, which presents a biochemical diagnostic marker for assessing the renal function [33]. The administration of vanadium complexes to diabetic rats led to normalization of the blood

urea and creatinine levels, indicating the recovered renal function is due to improved glycemic control.

Data on the hepatic glycogen levels in normal control and experimental groups of rats are demonstrated in Table 5. A decreased hepatic glycogen content in rats with STZ-induced diabetes was significantly restored ($P < 0.001$) after oral administration of vanadium complexes **3**, **5**, and **7** for 4 weeks, whereas no significant difference was observed in diabetic rats treated with the other complexes. Glycogen is formed by the conversion of excess glucose into glycogen under the influence of insulin, and is stored as energy fuel in tissues, predominantly in the liver and skeletal muscles. In case of diabetes, the reduced glycogen level in tissues is due to the insulin deficiency and/or impaired responsiveness of tissues to insulin [34]. In the present study, the improved liver glycogen content observed in diabetic rats treated with vanadium complexes indicates the effective glucose utilization and storage. Hepatic glucokinase catalyzes the conversion of glucose to glucose-6-phosphate, plays the central role in the maintenance of glucose homeostasis [35], and is considered to be a regulatory enzyme in the oxidation of glucose [36]. Since hepatic glucokinase is an insulin-dependent enzyme, its activity in diabetic rats is almost entirely inhibited or inactivated in the absence of insulin [37]. As shown in Table 5, the activity of hepatic glucokinase is significantly reduced in rats with STZ-induced diabetes as compared to the normal rats. This is mainly caused by the high glucagon/insulin ratio in STZ-treated animals. This reduction in the hepatic glucokinase activity in diabetic rats was significantly ameliorated in rats treated with vanadium complexes **3**, **5**, and **7**. In the present work, untreated diabetic rats showed significant decrease in the activity of hepatic glucokinase. This impairment resulted in a marked reduction in the rate of glucose oxidation via glycolysis, which ultimately led to hyperglycemia. Oral administration of vanadium complexes **3**, **5**, and **7** in rats with STZ-induced diabetes led to a significant recovery in the activity of glucokinase and thereby increased the oxidation of glucose. Insulin influences the intracellular utilization of glucose in a number of ways. Insulin increases hepatic glycolysis by increasing the activity and amount of several key enzymes. The insulin level in plasma was significantly decreased in diabetic rats because of the destruction of β -cells in pancreas, which inhibited insulin release (Table 5). Oral administration of vanadium complexes **3**, **5**, and **7** significantly increased the level of plasma insulin in rats with STZ-induced diabetes as compared to untreated diabetic control rats. These complexes stimulated the secretion of insulin from β -cells of pancreas. In hyperglycemic animals, it is possible that certain vanadium complexes may act by potentiating pancreatic insulin secretion or increasing glucose uptake [38].

Figure 5 shows the intensity of lipid peroxidation in different groups evaluated by the level of hepatic malondialdehyde (MDA). The results indicate that the hepatic MDA concentration exhibited five-fold increase in the STZ-treated

TABLE 5. Effect of Vanadium Complexes on the Levels of Hepatic Glycogen, Plasma Insulin and Glucokinase Activity in rats with STZ-induced diabetes

Group	Glycogen (mg/g)	Insulin (μ U/mL)	Glucokinase (U/mg)
Normal	13.6 \pm 2.1	18.3 \pm 1.4	57.6 \pm 8.9
STZ	4.1 \pm 1.3	8.1 \pm 0.3	14.3 \pm 1.4
STZ+1	4.3 \pm 0.5	6.3 \pm 0.4	18.5 \pm 3.1
STZ+2	5.8 \pm 1.5	7.3 \pm 0.6	11.4 \pm 1.5
STZ+3	11.6 \pm 3.1*	17.6 \pm 3.2*	53.6 \pm 6.1*
STZ+4	3.6 \pm 1.1	6.7 \pm 1.6	13.1 \pm 2.1
STZ+5	12.6 \pm 2.1*	16.9 \pm 2.4*	55.3 \pm 5.2*
STZ+6	3.9 \pm 1.4	7.4 \pm 1.8	15.6 \pm 1.5
STZ+7	14.6 \pm 3.1*	19.3 \pm 3.1*	61.7 \pm 7.3*

(*) Significant difference in comparison to diabetic rats.

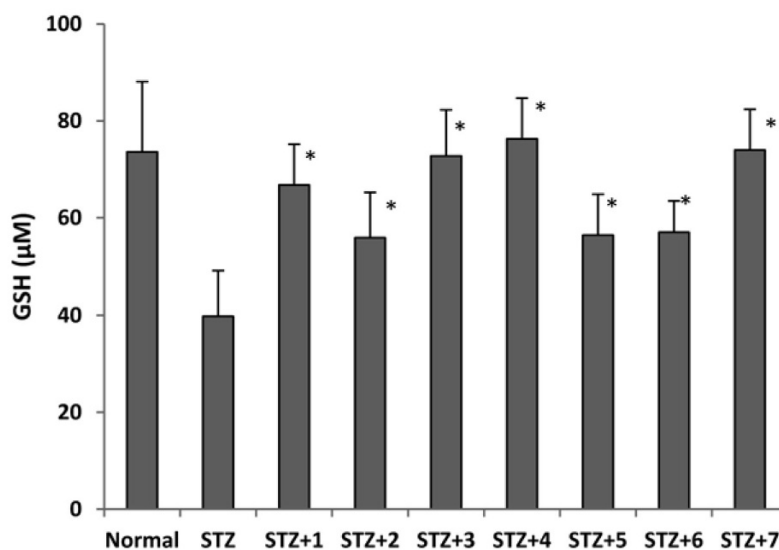


Fig. 6. Effect of vanadium complexes on the hepatic GSH level in rats with STZ-induced diabetes. (* significant difference when in comparison to diabetic rats).

group as compared to controls. The levels of hepatic MDA were significantly decreased in diabetic rats after treatment with vanadium complexes. Changes in the level of hepatic reduced glutathione (GSH) associated with hyperglycemia and diabetes, as well as the effects of vanadium complexes are shown in Figure 6. The hepatic GSH concentration was significantly decreased in rats with STZ-induced diabetes when compared to that in the controls. Furthermore, all vanadium-treated rats had a higher glutathione level in comparison to the diabetic group. These findings are in agreement with the result of Krośniak, et al. [39]. In a recent study [40], the levels of lipid peroxidation increased, whereas glutathione decreased as a result of its increased utilization due to oxidative stress, which was reversed by the administration of vanadyl sulfate in animals with STZ-induced diabetes.

4. CONCLUSION

In conclusion, the present study showed that the oral administration of vanadium(IV) complexes evoked marked blood glucose lowering effect in diabetic rats. The normalization of altered biochemical parameters in animals upon the treatment with vanadium complexes indicates the improved glucose homeostasis. Meanwhile, oxidative stress accompanied with diabetes was also modulated after treatment with vanadium complexes. The antidiabetic activity of vanadium complexes is structure-dependent and complexes **3**, **5**, and **7** exhibited potent antidiabetic properties, while the other complexes had no antihyperglycemic activity. Further study is recommended to establish the structure – activity relationship for vanadium complexes.

ACKNOWLEDGMENTS

The authors are thankful to the Scientific Research Deanship, Qassim University, KSA, for financially supporting research project number 1201 (2012).

REFERENCES

1. V. Sabetky and J. Ekblom, *Pharmacol. Res.*, **61**, 1 – 4 (2010).
2. American Diabetes Association: Diagnosis and Classification of Diabetes Mellitus, *Diabetes Care.*, **33**, S62 – S69 (2010).
3. Diabetes Mellitus: Reports of a WHO Study Group, *WHO Technical Report Series*, **727**, 876 (1985).
4. B. Ramachandran, D. S. Sekar, M. Kandaswamy, et al., *Exp. Diabetes Res*, **5**, 137 – 142 (2004).
5. B. Ramachandran, M. Kandaswamy, V. Narayanan, and S. Subramanian, *Diabetes Obes. Metab.*, **5**, 455 – 461 (2003).
6. B. Ramachandran, K. Ravi, V. Narayanan, et al., *Clin. Chim. Acta*, **345**, 141 – 150 (2004).
7. B. Ramachandran, K. Ravi, V. Narayanan, et al., *Chem. Biol. Interact.*, **149**, 9 – 21 (2004).
8. H. K. Thompson and C. Orvig, *J. Chem. Soc. Dalton Trans.*, 2885 – 2892 (2000).
9. H. Sakurai, H. Sano, T. Takino, and H. Yasui, *J. Inorg. Biochem.*, **80**, 99 – 105 (2000).
10. C. E. Heyliger, A. G. Tahiliani, and J. H. McNeill, *Science*, **227**, 1474 – 1477 (1985).
11. H. Degani, M. Gochin, S. J. D. Karlsh, and Y. Shechter, *Biochem.*, **20**, 5795 – 5799 (1981).
12. *Experimental Models of Diabetes*, J. H. McNeill (Ed.), CRC Press, Boca Raton (1999).
13. A. S. El-Tabl, F. A. El-Saied, W. Plass, and A. N. Al-Hakimi, *Spectrochim Acta Part A*, **71**, 90 – 99 (2008).
14. F. A. El-Saied, M. M. E. Shakhdofa, and A. N. Al-Hakimi, *J. Korean Chem. Soc.*, **55**, 444 – 453 (2011).

15. S. M. Emam, F. A. El-Saied, S. A. Abou El-Enein, and H. A. El-Shater, *Spectrochim. Acta Part A*, **72**, 291 – 297 (2009).
16. F. A. El-Saied, M. I. Ayad, R. M. Issa, and S. A. Aly, *Polish J. Chem.*, **75**, 773 – 783 (2001).
17. F. A. El-Saied, M. I. Ayad, R. M. Issa, and S. A. Aly, *Polish J. Chem.*, **74**, 919 – 926 (2000).
18. L. Lewis and R. G. Wilkins, *Modern Coordination Chemistry*, Interscience, New York (1960).
19. N. Rakieten, M. L. Rakieten, and M. V. Nadkarni, *Cancer Chemother. Rep.*, **29**, 91 – 98 (1963).
20. L. J. Fischer and D. E. Rickert, *CRC Crit. Rev. Toxicol.*, **3**, 231 – 263 (1975).
21. J. H. Roe and R. E. Dailey, *Anal. Biochem.*, **15**, 245 – 250 (1966).
22. E. Beutler, O. Duron, and M. B. Kelly, *J. Lab. Clin. Med.*, **61**, 882 – 888 (1963).
23. H. Ohkawa, A. Wakatsuki, and C. Kaneada, *Anal. Biochem.*, **95**, 351 – 358 (1982).
24. S. C. Jamdar and O. Greengard, *J. Biol. Chem.*, **245**, 2779 – 2783 (1970).
25. N. N. Greenwood, B. P. Straughan, and A. E. Wilson, *J. Chem. Soc. A*, 2209 – 2212 (1968).
26. M. H. Hamada, O. El-Shafai, and A. A. El-Asmy, *Trans. Met. Chem.*, **31**, 714 – 719 (2006).
27. A. A. El-Asmy, I. M. Gaber, N. M. El-Metwally, et al., *J. Coord. Chem.*, **61**, 3620 – 3633 (2008).
28. T. H. Rakha and M. M. Bekheit, *Chem. Pharm. Bull.*, **48**, 914 – 919 (2000).
29. S. I. Pillai, S. P. Subramanian, and M. Kandaswamy, *Eur. J. Med. Chem. C.*, **63**, 109 – 117 (2013).
30. M. van den Brand, L. D. Elving, J. P. Drenth, and J. H. van Krieken, *Neth. J. Med.*, **67**, 394 – 396 (2009).
31. N. Møller and K. S. Nair, *Diabetes*, **57**, 3 – 4 (2008).
32. P. H. Sugden and S. J. Fuller, *Biochem. J.*, **273**, 21 – 37 (1991).
33. H. Bräunlich, F. Marx, C. Fleck, and G. Stein, *Exp. Toxicol. Pathol.*, **49**, 135 – 139 (1997).
34. M. G. Bischof, M. Krssak, M. Krebs, et al., *Diabetes*, **50**, 392 – 398 (2001).
35. M. Laakso, M. Malkki, and S. Deeb, *Diabetes*, **44**, 330 – 334 (1995).
36. R. M. O'Doherty, D. L. Lehman, S. Telemaque-Potts, and C. B. Newgard, *Diabetes*, **48**, 2022 – 2027 (1999).
37. D. Gupta, J. Raju, J. Prakash, and N. Z. Baquer, *Diabetes. Res. Clin. Pract.*, **46**, 177 (1999).
38. P. Malini, G. Kanchana, and M. Rajadurai, *Asian J. Pharmaceut. Clin. Res.*, **4** (3), 124 – 128 (2011).
39. M. Krośniak, M. Gawlik, and R. Gryboś, *Bull. Vet. Inst. Pulawy*, **53**, 535 – 540 (2009).
40. T. Yilmaz-Ozden, O. Kurt-Sirin, S. Tunali, et al., *Bosn. J. Basic. Med. Sci.*, **14**(2), 105 – 109 (2014).